Int J Adv Manuf Technol (2011) 55:369–378
DOI 10.1007/s00170-010-3056-x

ORIGINAL ARTICLE

Mathematical modeling of a vehicle crash test based on elasto-plastic unloading scenarios of spring-mass models

Witold Pawlus · Hamid Reza Karimi · Kjell Gunnar Robbersmyr

Received: 27 September 2010 / Accepted: 21 November 2010 / Published online: 10 December 2010

Abstract This paper investigates the usability of spring which exhibit nonlinear force-deflection characteristic in the area of mathematical modeling of vehicle crash. We present a method which allows us to obtain parameters of the spring-mass model basing on the full-scale experimental data analysis. Since vehicle collision is a dynamic event, it involves such phenomena as rebound and energy dissipation. Three different spring unloading scenarios (elastic, plastic, and elasto-plastic) are covered and their suitability for vehicle collision simulation is evaluated. Subsequently we assess which of those models fits the best to the real car's behavior not only in terms of kinematic responses but also in terms of energy distribution.

Keywords Vehicle crash · Spring-mass model · Unloading stiffness · Coefficient of restitution · Total crash energy

1 Introduction

Vehicle users' safety is one of the great concerns of everyone who is involved in the automotive industry. Car manufacturers are obliged to perform variety of crash tests for every new type of car which is going to appear on the roads. However, such experiments, as one can easily assess, are complex and complicated—there are needed appropriate facilities, data acquisition systems, qualified staff—not to mention completely destroyed car. What is more, there is a long way to go from the design stage to the final prototype. For that reason, to verify whether a vehicle satisfies the initial safety requirements, such an expensive test has to been conducted in different car design phases. Therefore it is advisable to establish a vehicle crash model and use its results instead of a full-scale experiment measurements to predict car's behavior during a collision.

Nowadays, we can distinguish two main approaches in this area. The first one utilizes finite element method (FEM) software: car's model is created in computer-aided design (CAD) program and subsequently mesh is applied to it, structural parameters are assigned and impact conditions are specified. The second method is called lumped parameter modeling (LPM). It consists in formulating equations of motion of viscoelastic systems (arrangements of springs, dampers and masses in different configurations) and solving them to precisely determine models' responses. There is a number of methods which can be applied to assess parameters of such models (stiffness, damping) basing on the real crash data. One of them is fitting the real car's displacement to the models' responses—see [1, 2], and [3].

Because of the fact that crash pulse is a complex signal, it is justified to simplify it. One solution for this is covered in [4]. Wavelet-based approximation of the crash pulse can be used to perform its analysis: accuracy of this method is very good. References [5, 6], and [7]

W. Pawlus · H. R. Karimi (✉) · K. G. Robbersmyr
Faculty of Engineering and Science, University of Agder, Postboks 509, 4898 Grimstad, Norway
e-mail: hamid.r.karimi@uia.no

W. Pawlus
e-mail: witolp09@student.uia.no

K. G. Robbersmyr
e-mail: kjell.g.robbersmyr@uia.no

talk over commonly used ways of describing a collision, e.g., investigation of tire marks or the crash energy approach.

Vehicle crash investigation is an area of up-to-date technologies application. References [8, 9], and [10] discuss usefulness of such developments as neural networks or fuzzy logic in the field of modeling of crash events. Those two intelligent technologies have extremely high potential for creation of vehicle collision dynamic models and their parameters establishment—e.g., in [11] the values of spring stiffnesses and damping coefficients for LPM were determined by the use of radial basis artificial neural network and the responses generated by such models were compared with the ones obtained via analytical solutions. Fuzzy logic together with neural networks and image processing have been employed in [12] to estimate the total deformation energy released during a collision.

In the most recent scope of research concerning crashworthiness it is to define a dynamic vehicle crash model which parameters will be changing according to the changeable input (e.g., initial impact velocity). One of such trials is presented in [13]—a nonlinear occupant model is established and scheduling variable is defined to formulate linear parametrically varying model. In addition to this work, in [14] one can find a complete derivation of vehicle collision mathematical models composed of springs, dampers and masses with piecewise nonlinear characteristics of springs and dampers. What is also relevant to the topic of this paper, is the methodology included in [15]. Comparative analysis of vehicle collision models established using so called response surface methodology (RSM) and radial basis functions (RBF) is shown there. The obtained results have confirmed that RSM is able to produce good approximation models for energy absorption, however, in the case of peak acceleration, RBF is found to generate better models than RSM based on the same number of response samples.

As in the case of a vehicle crash simulation, here we can also distinguish two main ways of examining the occupant behavior during an impact. Reference [16] focuses on finding the relationship between the car's damage and occupant injuries. On the other hand, [17] employs FEM software to closely study the crash severity of particular body parts.

What plays an important role in increasing traffic safety, is also investigation of pedestrian safety and modeling accidents in which those vulnerable road users are involved. Reference [18] investigates heterogeneity of pedestrians injuries. A mixed logit model has been applied in this research. It allowed to determine what the relationships are between crash severity of pedestrians and their unobservable features, like physical health, strength and behavior. It is of key importance to relate crash occurrence with roadway design features too. In [19], a multivariate Poisson-lognormal specification is presented, that simultaneously models crash counts by injury severity. The results of such approach are useful for recommendations for highway safety treatments and design policies.

The main contribution of this paper is the evaluation of the presented methods with the full-scale experimental data. We show that even the basic spring-mass model can give us reliable and reasonable results if we only manipulate its stiffness in the unloading phase. Application of the spring which has a nonlinear force-deflection characteristic is a considerable improvement to the vehicle crash mathematical model. Establishment of parameters of an elasto-plastic spring allows us to assess that the mid-speed vehicle to pole collision can be satisfactorily represented just by the spring with plastic unloading properties.

In this paper, we present an analysis of the vehicle crash event by introducing the energy concept. We investigate a simple spring-mass model with different unloading scenarios. The data used by us has been taken from the full-scale experiment elaborated in [20]. By integrating the measured acceleration in the time interval corresponding to the collision duration, we obtain the reference car's displacement. Then we establish our model's spring stiffnesses for loading and three unloading cases. By doing so we are able to simulate behavior of elastic, plastic and elasto-plastic spring. For each of those models, we calculate the total crash energy and determine their kinematic responses (acceleration, velocity and displacement) as well as plot their force-deflection characteristics. In the end, we present conclusions concerning application of different loading and unloading stiffness of spring in the simple spring-mass model.

2 Spring-mass model

Scheme of this system is shown in Fig. 1. Its motion is a nondecayed oscillatory one (sinusoidal) because there is no damping in it. Let us define the following notation:

- k - spring stiffness (N/m)
- m - mass (kg)
- v - initial impact velocity (m/s)
- α - model's displacement (m).

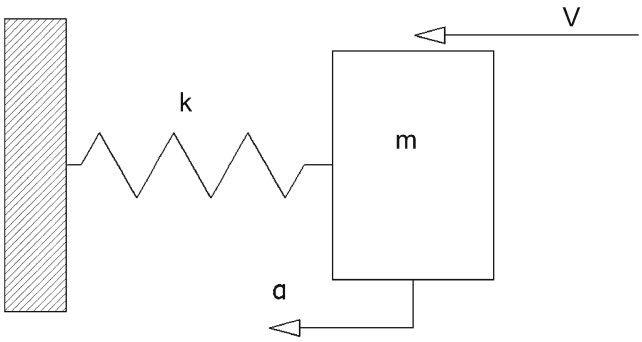

Fig. 1 Spring-mass model

2.1 Model's kinematics

Since motion of the system is sinusoidal, its transient responses (displacement, velocity, and acceleration, respectively) are given by the following formulas:

$$\alpha(t) = \frac{V}{\omega_e} \sin(\omega_e t) \tag{1}$$

$$\dot{\alpha}(t) = V \cos(\omega_e t) \tag{2}$$

$$\ddot{\alpha}(t) = -V\omega_e \sin(\omega_e t). \tag{3}$$

Furthermore, we define maximum dynamic crash, time when it occurs, and circular natural frequency, respectively:

$$C = \frac{V}{\omega_e} \tag{4}$$

$$t_m = \frac{\pi}{2\omega_e} \tag{5}$$

$$\omega_e = \sqrt{\frac{k}{m}} \tag{6}$$

where:

- V - initial barrier impact velocity (m/s)
- k - spring stiffness (N/m)
- m - vehicle's mass (kg).

2.2 Model's establishment

To investigate what the parameters C and t_m of such a model are, we need to find spring stiffness k. By substituting Eqs. 6 to 4 and rearranging we get:

$$k = \frac{V^2}{C^2} m. \tag{7}$$

Please note that Eq. 7 allows us to obtain such stiffness k which satisfies just the dynamic crash condition. When it comes to the time when it occurs t_m, it can be checked by Eq. 5.

2.3 Model's dynamics

In the most general case, a typical spring exhibits elasto-plastic properties. It means that it has at least two different values of spring stiffness (one for loading and the other one for unloading). Force-deflection data for such a spring is shown in Fig. 2.

Let us introduce the following notation:

- d_c - dynamic crash
- d_p - permanent deformation
- d_e - elastic rebound displacement ($d_e = d_c - d_p$)
- F_1 - force at d_c
- k_L - loading stiffness
- k_U - unloading stiffness
- ΔE - total crash energy absorbed at c
- $\Delta E'$ - elastic energy recovered
- v - vehicle impact speed
- v' - vehicle rebound velocity
- e - coefficient of restitution (COR).

Figure 2 shows the special case of spring deformation procedure in which its permanent deformation is achieved (intercept of the unloading slope k_U on the zero force level). We can distinguish the following three types of springs, depending on the value of the unloading stiffness k_U:

1. Elastic: $k_U = k_L$—no energy dissipation, spring returns to its initial position
2. Plastic: $k_U = \infty$—whole energy absorbed is dissipated, no rebound, maximum deflection is at the same time permanent deformation ($d_c = d_p$)
3. Elasto-plastic: $k_U > k_L$—dissipated energy is equal to the triangle-like area from Fig. 2: area under force-deflection curve in loading phase minus area under force-deflection curve in unloading phase, spring achieves permanent deformation after the rebound.

Remark 2.1 If $k_U < k_L$, there is no rebound—i.e., the spring is still in the loading phase.

The following relationships are established to define dependency between linear loading stiffness k_L and linear unloading stiffness k_U (see [21]):

$$F_1 = k_L d_c = k_U d_e \text{—maximum spring force at } d_c \tag{8}$$

$$\frac{d_e}{d_c} = \frac{k_L}{k_U} \tag{9}$$

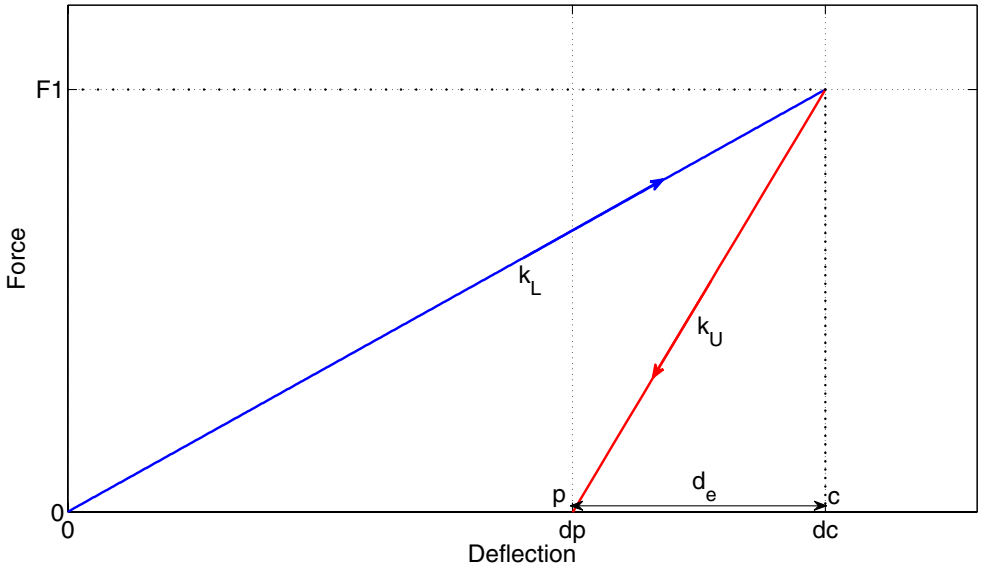

Fig. 2 Force-deflection characteristic of an elasto-plastic spring

$$\Delta E = \frac{1}{2}k_L d_c^2 = \frac{1}{2}mv^2\text{—}\textit{crash energy absorbed at } d_c \tag{10}$$

$$\Delta E' = \frac{1}{2}k_U d_e^2 = \frac{1}{2}mv'^2\text{—}\textit{rebound energy} \tag{11}$$

$$\frac{\Delta E'}{\Delta E} = \left(\frac{v'}{v}\right)^2 = e^2 \tag{12}$$

$$\Delta E_d = \Delta E - \Delta E' = \Delta E(1 - e^2)\text{—}\textit{energy dissipated} \tag{13}$$

$$\frac{\Delta E'}{\Delta E} = \frac{k_U d_e^2}{k_L d_c^2}. \tag{14}$$

By substituting Eqs. 9 and 12 into Eq. 14 we obtain:

$$e^2 = \frac{k_L}{k_U} \tag{15}$$

$$k_U = \frac{k_L}{e^2} \tag{16}$$

$$e = \sqrt{\frac{d_e}{d_c}} \tag{17}$$

It is shown that the ratio of linear spring stiffnesses in two different modes (loading and unloading) is equal to the COR squared. Coefficient of restitution is equal to zero for perfectly plastic crash ($k_U = \infty$) and equal to one for perfectly elastic crash ($k_U = k_L$).

Fig. 3 Subsequent steps of crash test

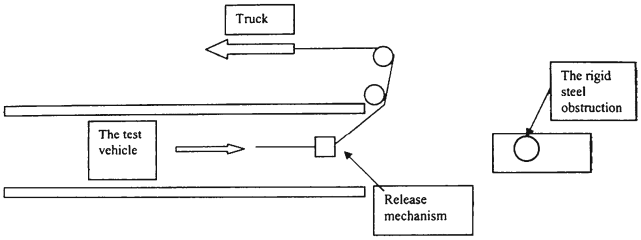

Fig. 4 Experiment procedure

3 Experimental setup description

The data which we use come from the typical vehicle to pole collision—the sequence of the crash is illustrated in Fig. 3.

A test vehicle was subjected to impact with a vertical, rigid cylinder. During the test, the acceleration was measured in three directions (longitudinal, lateral, and vertical) together with the yaw rate from the center of gravity of the car. The acceleration field was 100-m long and had two anchored parallel pipelines. The pipelines have a clearance of 5 mm to the front wheel tires. The force to accelerate the test vehicle was generated using a truck and a tackle. The release mechanism was placed 2 m before the end of the pipelines and the distance from there to the test item was 6.5 m. The vehicle was steered using the pipelines that were bolted to the concrete runaway. The experiment scheme is shown in Fig. 4.

3.1 Description of the car and pole

The initial velocity of the car was 35 km/h, and the mass of the vehicle (together with the measuring equipment and dummy) was 873 kg. When it comes to the pole (obstruction), it was constructed with two components: a baseplate and a pipe. Both of them were made of steel. The baseplate had dimensions 740 × 410 × 25 mm. The pipe had length 1,290 mm and overall diameter equal to 275 mm. The obstruction pipe was filled with concrete and mounted on a concrete foundation with five bolts. These bolts connected the concrete foundation with the baseplate of the obstruction which was fixed to the shovel of a bulldozer—see Fig. 5.

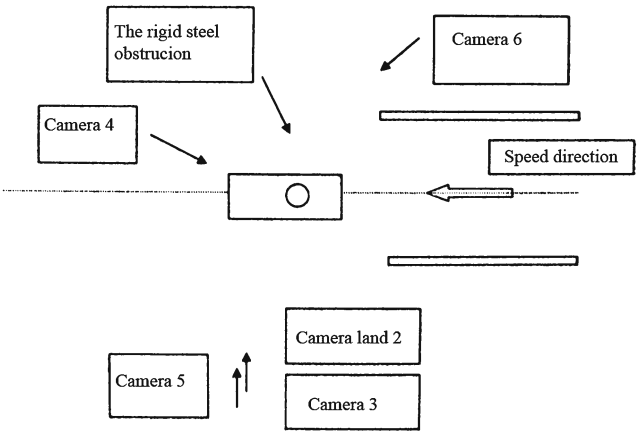

Fig. 6 Layout of the cameras in the crash test

3.2 Instrumentation

During the test, the acceleration at the center of gravity in three dimensions (x-longitudinal, y-lateral, and z-vertical) was recorded. The vehicle speed before the collision was measured. The yaw rate was also measured with a gyro meter. Using normal speed and high—speed video cameras, the behavior of the safety barrier and the test vehicle during the collision was recorded—video recorders' arrangement is presented in Fig. 6.

3D accelerometer was mounted on a steel bracket close to the vehicle's center of gravity and the bracket was fastened by screws to the vehicle's chassis. The yaw rate was measured with a gyro instrument which makes it is possible to record 1°/s. Data from the sensor was fed to an eight channel data logger and subsequently sampled with a frequency of 10 kHz. The memory was able to store 6.5 s of data per channel. The velocity of

Fig. 5 Obstruction

Fig. 7 Car's deformation

the vehicle was checked by an inductive monitor. It was directed towards a perforated disc mounted on a wheel on the right side of the test vehicle. Figure 7 shows the car before, during and after the collision.

3.3 Crash pulse analysis

Having at our disposal the acceleration measurements from the collision, we are able to describe in details motion of the car. Since it is a central impact, we analyze only the pulse recorded in the longitudinal direction (x-axis). By integrating the car's deceleration, we obtain plots of velocity and displacement, respectively—see Fig. 8.

At the time when the relative approach velocity is zero, the maximum dynamic crash occurs. The relative velocity in the rebound phase then increases negatively up to the final separation (or rebound) velocity, at which time a vehicle rebounds from an obstacle. The contact duration of the two masses includes both contact times in deformation and restitution phases. When the relative acceleration becomes zero and relative separation velocity reaches its maximum recoverable value we have the separation of the two masses. From the crash pulse analysis, we obtain the data listed in Table 1.

4 Models establishment

With all the knowledge coming form the theoretical considerations and full-scale experiment's analysis, we proceed to the formulation of spring-mass models for three different unloading scenarios. Taking advantage of Eqs. 7 and 5, we determine the value of loading stiffness and time when the maximum dynamic crash occurs to be $k_L = \frac{(9.86\ \text{m/s})^2}{(0.52\ \text{m})^2} \cdot 873\ \text{kg} = 313,878\ \text{N/m}$ and $t_m = \frac{\pi}{2 \cdot 18.96\ \text{rad/s}} = 83\ \text{ms}$, respectively.

Remark 4.1 It is noting that all the modeling presented in this paper is conducted according to the crash pulse analysis only in the x-direction (longitudinal). Such

Fig. 8 Car's kinematics

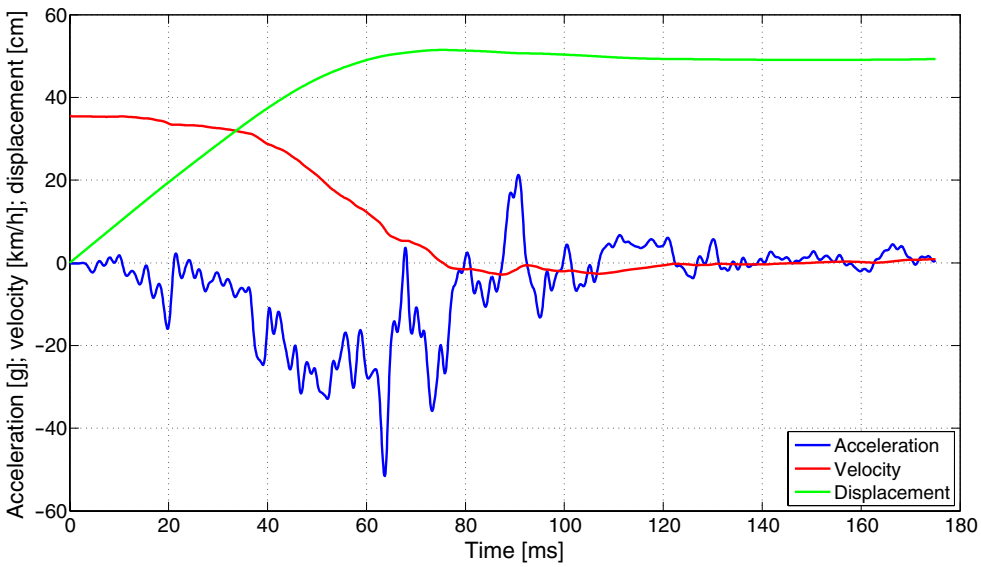

Table 1 Crash test parameters

Parameter	V (m/s)	V' (m/s)	e	d_c (cm)	d_p (cm)	t_m (ms)	ΔE (kJ)	$\Delta E'$ (kJ)
Value	9.86	1.96	0.2	52	50	76	42.44	1.68

application of the spring-mass model is simple and does not require any additional considerations related to the two or three dimensional modeling (as in the case of e.g., angular impact). When it comes to modeling such a nonfrontal crash event (or e.g., an offset impact), it is advisable to provide possibility of model's motion in two dimensions. This can be achieved by application of e.g., two springs being connected to the model perpendicularly to each other. Such constraint will results in making possible simulation of car's movement in two axes. However, it would be more complex to precisely evaluate the car's deformation, since the acceleration's integration will give us only the car's displacement, not the intrusion to the passenger's compartment (only in the particular case—frontal impact—dynamic crash is equal to the car's displacement).

4.1 Elastic unloading

Since $k_U = k_L$ there are no energy losses in this type of simulation. The collision modeled is perfectly elastic, therefore the rebound velocity is equal to the initial impact velocity ($V' = V$ as well as $\Delta E = \Delta E'$). Figure 9 shows force-deflection characteristic of this type of event as well as its kinematic responses.

4.2 Plastic unloading

Since $k_U = \infty$, the total crash energy is completely dissipated. The collision modeled is perfectly plastic, therefore there is no rebound—when a mass reaches the maximum displacement, it stops. Figure 10 shows force-deflection characteristic of this type of event as well as its kinematic responses. Please note that the area under the force-deflection curve is exactly equal to the dissipated kinetic energy.

4.3 Elasto-plastic unloading

This type of event is of our main interest, since it describes a system in which rebound occurred (together with the energy dissipation). Using Eq. 16 we determine the unloading spring stiffness which is found to be $k_U = 7{,}846{,}950$ N/m. Due to the absence of a damper, the change of stiffness will result in change of only a period and an amplitude of mass oscillations. Therefore,

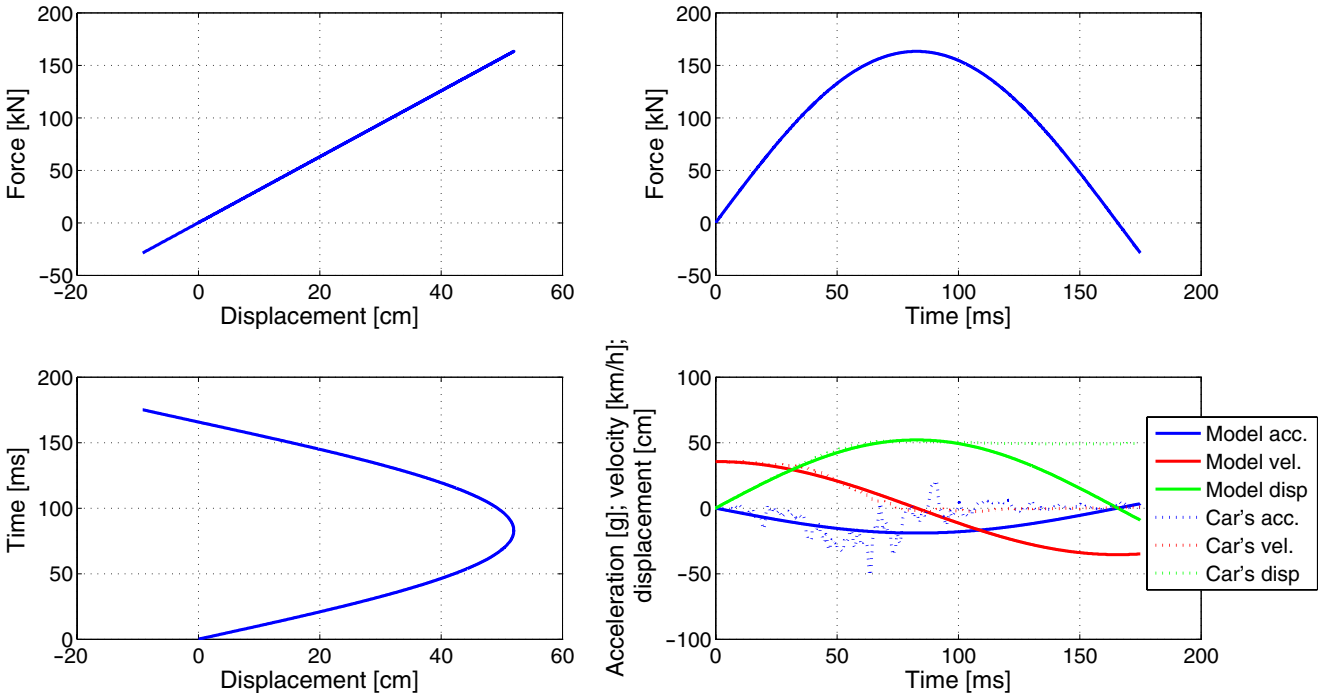

Fig. 9 Elastic spring-mass model simulation results

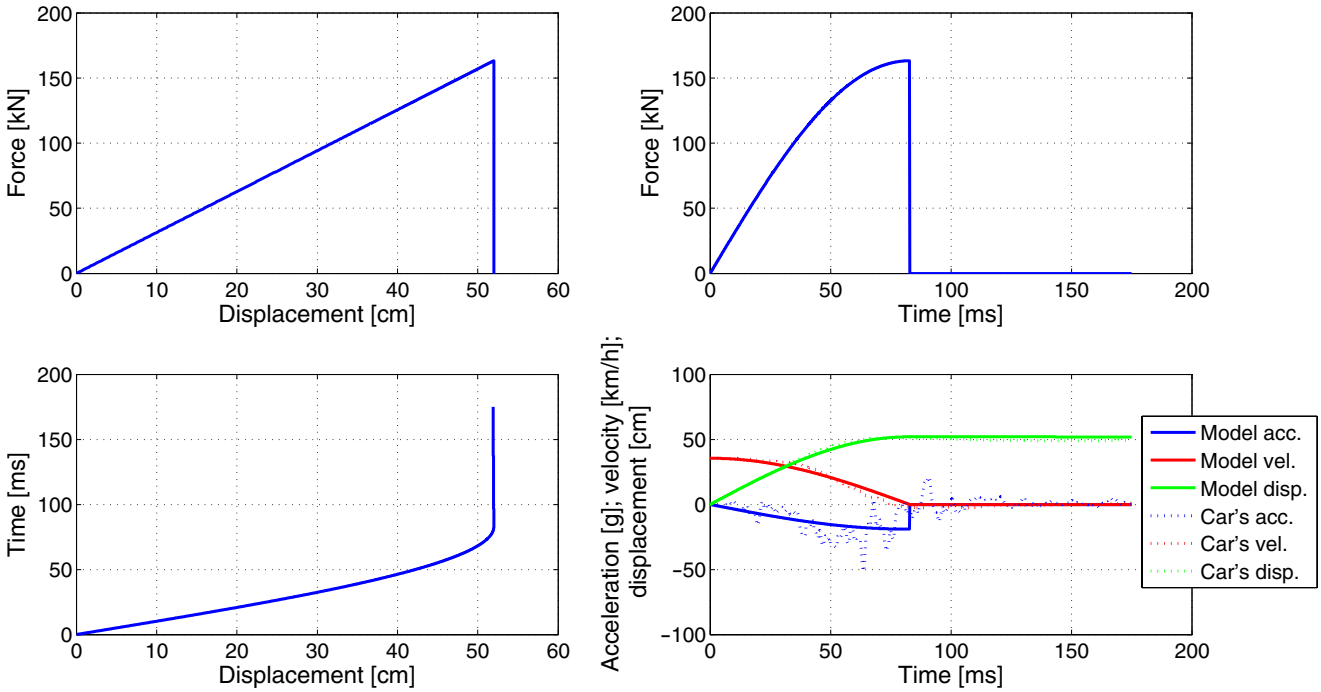

Fig. 10 Plastic spring-mass model simulation results

system's motion would still be nondecayed and oscillatory. Hence, for the simplification purposes we assume that in our spring-mass model there occurs only one loading and only one unloading—we do not consider reloading of the spring. That is why parts of the graphs depicting spring oscillations after those two events are beyond the scope of our analysis—they present the expected spring-mass system's behavior after the change

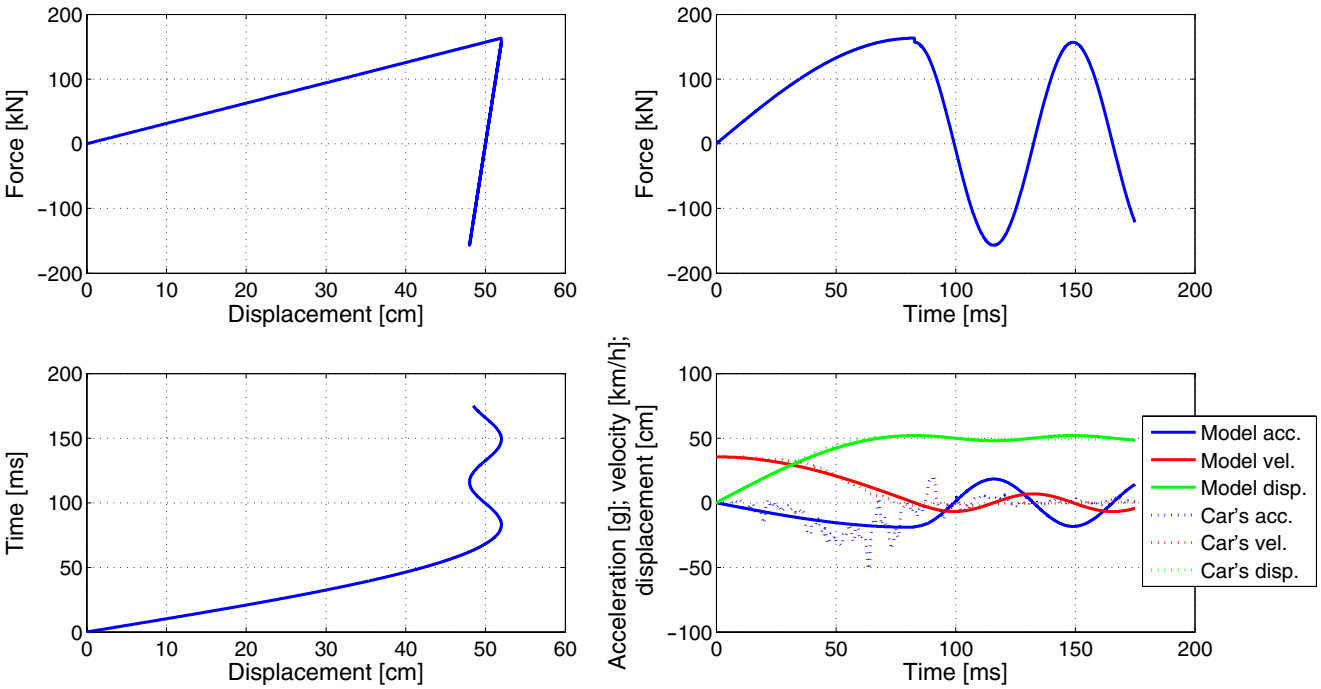

Fig. 11 Elasto-plastic spring-mass model simulation results

Table 2 Comparative analysis of three unloading scenarios

Parameter	Elastic	Plastic	Elasto-plastic
Loading stiffness (k_L (N/m))	313,878	313,878	313,878
Unloading stiffness (k_U (N/m))	313,878	∞	7,846,950
Total crash energy (ΔE kJ)	42.44	42.44	42.44
Rebound energy ($\Delta E'$ kJ)	42.44	0	1.68
COR (e)	1	0	0.2
Elastic rebound (e^2 (%))	100	0	4
Kinetic energy dissipated ($(1-e^2)$ (%))	0	100	96

of its parameters—so they are just results of simulation of a theoretical element. Figure 11 presents the outcome of model's validation.

As we see, during the first cycle (i.e., the first loading and the first unloading, from Fig. 11 we determine that time to be 100 ms), the spring force dropped to zero, forming triangle-like force-deflection characteristics (i.e., this area corresponds to the kinetic energy dissipated in the crash) and the displacement reached the permanent deformation value $d_p = 50$ cm. The further simulation results illustrate the responses of the totally underdamped model. Admittedly, they are correct but they do not follow our assumption of only one loading and one unloading. Our simulation ends when the mass reaches the displacement corresponding to the permanent deformation $d_p = 50$ cm (simulation duration is 100 ms).

5 Simulation results

Table 2 shows the values of main parameters describing the performance of models. Please note that in all of those three cases, the total crash energy is the same $\Delta E = 42.44$ kJ. Let us introduce two new helpful factors: elastic rebound (e^2 (%)), which designates what the percentage of the displacement in the rebound phase is and kinetic energy dissipated ($(1-e^2)$, (%)) obtained from Eq. 13, which determines the percentage of energy loss during the collision.

From Table 2 we conclude that the vehicle to pole collision which we deal with can be represented by the spring with totally plastic behavior. That is because the values of elastic rebound e^2 and energy recovered in the rebound phase $\Delta E'$ are relatively low for the elasto-plastic spring. However, elasto-plastic spring gives us the full insight into the nature of vehicle crash event in which the rebound (even small) occurs.

6 Conclusions

In this paper, we have presented an analysis of a spring-mass model with different values of stiffness for loading and unloading phases. Results confirmed that this approach provides reasonable results. Vehicle to pole collision is a type of event which consumes a lot of energy due to the localized impact—in another words, it produces less rebound than a corresponding vehicle to rigid barrier collision. For that reason, it is sufficient to simulate such a crash with a spring which demonstrates plastic behavior in the restitution phase. Method presented by us is simple and gives reasonable results. However, to represent in details car's behavior, it is advisable to use a spring which exhibit elasto-plastic properties. Therefore in our future work we will improve this model by establishing a couple of unloading stiffnesses making it possible to simulate the reload of the system more accurately. Apart from that, adding a damper (energy dissipation element) to the assembly will increase model's fidelity—as well as applying springs with nonlinear characteristics since most of the real world materials exhibit nonlinear force-deflection performance.

References

1. Pawlus W, Nielsen JE, Karimi HR, Robbersmyr KG (2010) Mathematical modeling and analysis of a vehicle crash. In: The 4th European computing conference, Bucharest, Romania
2. Pawlus W, Nielsen JE, Karimi HR, Robbersmyr KG (2010) Development of mathematical models for analysis of a vehicle crash. WSEAS Trans Appl Theor Mech 5(2):156–165
3. Pawlus W, Nielsen JE, Karimi HR, Robbersmyr KG (2010) Further results on mathematical models of vehicle localized impact. In: The 3rd international symposium on systems and control in aeronautics and astronautics, Harbin, China
4. Karimi HR, Robbersmyr KG (2010) Wavelet-based signal analysis of a vehicle crash test with a fixed safety barrier. In: WSEAS 4th European computing conference, Bucharest, Romania
5. Šušteršič G, Grabec I, Prebil I (2007) Statistical model of a vehicle-to-barrier collision. Int J Impact Eng 34(10):1585–1593
6. Trusca D, Soica A, Benea B, Tarulescu S (2009) Computer simulation and experimental research of the vehicle impact. WSEAS Trans Comput 8(1):1185–1194
7. Vangi D (2009) Energy loss in vehicle to vehicle oblique impact. Int J Impact Eng 36(3):512–521

8. Giavotto V, Puccinelli L, Borri M, Edelman A, Heijer T (1983) Vehicle dynamics and crash dynamics with minicomputer. Comput Struct 16(1):381–393
9. Harmati IA, Rovid A, Szeidl L, Varlaki P (2008) Energy distribution modeling of car body deformation using LPV representations and fuzzy reasoning. WSEAS Trans Syst 7(1):1228–1237
10. Omar T, Eskandarian A, Bedewi N (1998) Vehicle crash modelling using recurrent neural networks. Math Comput Model 28(9):31–42
11. Pawlus W, Nielsen JE, Karimi HR, Robbersmyr KG (2010) Comparative analysis of vehicle to pole collision models established using analytical methods and neural networks. In: The 5th IET international system safety conference, Manchester, UK
12. Várkonyi-Kóczy AR, Rövid A, Várlaki P (2004) Intelligent methods for car deformation modeling and crash speed estimation. In: The 1st Romanian–Hungarian joint symposium on applied computational intelligence, Timisoara, Romania
13. van der Laan E, Veldpaus F, de Jager B, Steinbuch M (2008) LPV modeling of vehicle occupants. In: AVEC '08 9th international symposium on advanced vehicle control, Kobe, Japan
14. Elmarakbi AM, Zu JW (2006) Crash analysis and modeling of two vehicles in frontal collisions using two types of smart front-end structures: an analytical approach using IHBM. Int J Crashworthiness 11(5):467–483
15. Fang H, Rais-Rohani M, Liu Z, Horstemeyer MF (2005) A comparative study of metamodeling methods for multiobjective crashworthiness optimization. Comput Struct 83(25–26):2121
16. Conroy C, Tominaga GT, Erwin S, Pacyna S, Velky T, Kennedy F, Sise M, Coimbra R (2008) The influence of vehicle damage on injury severity of drivers in head-on motor vehicle crashes. Accident Anal Prev 40(4):1589–1594
17. Niu Y, Shen W, Stuhmiller JH (2007) Finite element models of rib as an inhomogeneous beam structure under high-speed impacts. Med Eng Phys 29(7):788–798
18. Kim JK, Ulfarssonn GF, Shankar VN, Mannering FL (2010) A note on modeling pedestrian-injury severity in motor-vehicle crashes with the mixed logit model. Accident Anal Prev 42(6):1751–1758
19. Ma J, Kockelman KM, Damien P (2008) A multivariate Poisson-lognormal regression model for prediction of crash counts by severity, using Bayesian methods. Accident Anal Prev 40(3):964–975
20. Robbersmyr KG (2004) Calibration test of a standard ford fiesta 1.1l, model year 1987, according to NS - EN 12767. Technical Report 43/2004, Agder Research, Grimstad
21. Huang M (2002) Vehicle crash mechanics. CRC Press, Boca Raton